Measurements and analysis of active/passive multispectral imaging

Christina Grönwall[1a], Dominique Hamoir[b], Ove Steinvall[a], Håkan Larsson[a], Elias Amselem[a], Peter Lutzmann[c], Endre Repasi[c], Benjamin Göhler[c], StéphaneBarbé[d], Olivier Vaudelin[b], Michel Fracès[b], Bernard Tanguy[b], Emmanuelle Thouin[b]
[a]FOI (Swedish Defence Research Agency), P.O. Box 1165, 583 11 Linköping, Sweden
[b]ONERA – The French Aerospace Lab, F-31055 Toulouse, France
[c]Fraunhofer IOSB, Gutleuthausstrasse 1, 76275 Ettlingen, Germany
[d]ONERA – The French Aerospace Lab, F-13661 Salon de Provence, France

ABSTRACT

This paper describes a data collection on passive and active imaging and the preliminary analysis. It is part of an on-going work on active and passive imaging for target identification using different wavelength bands. We focus on data collection at NIR-SWIR wavelengths but we also include the visible and the thermal region. Active imaging in NIR-SWIR will support the passive imaging by eliminating shadows during day-time and allow night operation. Among the applications that are most likely for active multispectral imaging, we focus on long range human target identification. We also study the combination of active and passive sensing. The target scenarios of interest include persons carrying different objects and their associated activities. We investigated laser imaging for target detection and classification up to 1 km assuming that another cueing sensor – passive EO and/or radar – is available for target acquisition and detection. Broadband or multispectral operation will reduce the effects of target speckle and atmospheric turbulence. Longer wavelengths will improve performance in low visibility conditions due to haze, clouds and fog. We are currently performing indoor and outdoor tests to further investigate the target/background phenomena that are emphasized in these wavelengths. We also investigate how these effects can be used for target identification and image fusion. Performed field tests and the results of preliminary data analysis are reported.

Keywords: Range-gated imaging, burst illumination, laser signatures, human signatures, thermal imaging, active imaging, multi-spectral imaging, multi-sensor imaging

1. INTRODUCTION

Based on the results from the EDA OB study ACTIM 2010-11 [1, 2, 3], Onera (France), Fraunhofer-IOSB (Germany) and FOI (Sweden) have agreed upon the importance of live demonstrating the benefits of active imaging, and of multi-spectral active imaging, as a complement to passive imaging. Laser imaging offers a great number of capabilities like 3D imaging, penetration through fog, haze and smoke as well as preserving a high target to background contrast. On the other hand, great progress has recently occurred in passive multi- and hyper-spectral imaging with applications ranging from environmental monitoring and geology to mapping, military surveillance, and reconnaissance. Data bases on spectral signatures allow the possibility to discriminate between different materials in the scene. While passive multi or hyper spectral sensors rely on direct or indirect solar radiation, active spectral sensors have the advantage of controlling the illumination. It is therefore of interest to extend spectral imaging to also include active sensing, especially for target identification (ID).

While the literature on passive spectral imaging is rich, it is much more limited for active spectral sensing. An early example of such a sensor was the Lincoln Laboratory "Multispectral Active/Passive Sensor (MAPS)", which included active pulsed laser illumination at 0.85 μm and 10.59 μm, as well as an 8-to-12μm thermal imager [4]. More recent work from MIT extends the active image concept to the hyperspectral regime using white-light pulsed laser for illumination [5]. Other examples include both polarimetric and multispectral active imaging [6,7,8, 9].

[1]christina.gronwall@foi.se, www.foi.se

Electro-Optical Remote Sensing, Photonic Technologies, and Applications VII; and Military Applications in Hyperspectral Imaging and High Spatial Resolution Sensing, edited by G. W. Kamerman, O. K. Steinvall, G. J. Bishop, J. D. Gonglewski, Proc. of SPIE Vol. 8897, 889705 · © 2013 SPIE · CCC code: 0277-786X/13/$18 · doi: 10.1117/12.2028647

A recent interesting experiment using a multi-spectral mid-infrared laser stand off imager was reported by Wang et al. [10]. The system was applied to diverse targets that consist of man-made and natural materials and objects, and shown capable to resolve and distinguish small spectral differences among the various targets. Colourless objects in the visible were shown with "colourful" signatures in the mid-IR. Stothard et al. [11] demonstrated a system for the active real-time hyperspectral imaging of gases as well as liquids [12] of a compact, pump-enhanced, continuous-wave optical parametric oscillator as an all-solid-state midinfrared source of coherent radiation and an electro-mechanical polygonal imager. A danish group have also demonstrated multispectral 3-D imaging [13]. By exploiting Raman scattering in single-mode optical fibers, multispectral light was generated from a green nanolaser with a high pulse repetition rate.

Powers et al. [14, 15] present a ladar for UGV (unmanned ground vehicle) applications for a combined ATR (automatic target recognition) function using a combination of spectral and spatial imaging. The results are discussed here in the context of autonomous vehicle navigation and target recognition. Applying a broadband source in airborne lidar allows multi- or hyper-spectral classification of the objects and topography including water and sea flooreven at night time. Kaasalainen et al. [16] and Hakala et al. [17] have made laboratory investigations of backscattter properties using a supercontinuum source. Park et al. obtaines absolute scene reflectivity by multispectral imaging using time multiplexed LED illumination [18].

Today's mixed battlefield with soldiers, combatants and civilians accentuate the need for the recognition of individuals, handheld objects and associated activities at rather long ranges and in diversified environments. Examples of investigations of target recognition tasks include handheld weapons [19,20]. These investigations were made at close ranges in the laboratory using visible and thermal imaging. Turbulence was indirectly treated as the pixels were blurred. However treatment of turbulence blur as a single MTF neglects the significant variations in spatial blur and temporal blur which is connected with the atmospheric propagation. Krapelset al. [21] discuss atmospheric turbulence modulation transfer function for infrared target acquisition modeling. Espinolaet al. [22] use a controlled human perception test to assess handheld weapon identification performance before and after turbulence mitigation post processing. The U.S. Army's infrared and active imaging target acquisition models including the Target Task Performance (TTP) metric involves discrimination criteria for human targets and handheld objects [23,24,25].

Farley et al. investigated the soldier's camouflage equipment using multispectral and hyperspectralsensing [26] and Zhou et al. [27] describes camouflaged target detection based on visible and near infrared polarimetric imagery fusion. Hogervorstet al.[28] evaluates urban camouflage using human observers.

Recognition of human activities by automated analysis of video sequences has been a subject of great attention during recent years. Turagaet al. [29] give a survey of machine recognition of human activities. In the military application, an observer is very often involved especially if the activities are suspected to be hostile. O'Connor et al. [30] assessed spatial and motion characteristics of man targets to investigate the potential of hostile intentions. Steinvall et al. [31,32] investigated identification of handheld objects and human activities in active and passive imaging operating in the NIR and SWIR regions and also compared that with imagery from a thermal imaging camera. Adomeit [33] presents handheld object identification using thermal cameras.

In this paper both active and passive imaging for target ID using different wavelength bands is reported. Our first objective is to distinguish people against rural and urban backgrounds. The second objective is to distinguish their clothes, hand-held objects and activities in order to allow Friend/Foe identification and to perform efficient monitoring of the situation. We will evaluate the performance of individual active and passive EO sensors and sensor combinations in these tasks. A focus is set on the added value of active imaging when combined to passive imaging, as well as on the interest of multispectral imaging. The paper starts with a description of the trial followed by example of collected data. A preliminary analysis is shown on a subset of the data. Finally there is a discussion with future prospects.

2. TRIAL DESCRIPTION AND INSTRUMENTS (SW)

2.1 General description

The field trial was conducted on the Pirrène laser range of Onera, Mauzac site in South of France, 8th-12th April 2013. Participating research groups were Onera (France), Fraunhofer-IOSB (Germany) and FOI (Sweden). The laser range of Onera offers a measurement range of 1040 m (Figure 1) and is about 25 m wide. The open field consists mostly of grass, with low bushes on one side of the field and trees on the other side. As the campaign was performed under the spring season in South France, leaves and grass had started to grow. Scenarios were played at ranges from 600 m up to 1000 m.

Variations include the environment (weather, ambient light, turbulence), target ranges (600-1000 m), foreground and background (vegetation, concrete), and first of all target features (type of clothes, handheld objects, morphology, posture, activity).

The goal in this campaign was thus to combine several passive and active imaging modalities, in as many spectral bands as possible (VIS, NIR, SWIR, MWIR and LWIR), to recognise human activities and human targets, including their handheld objects. The features of interest are the reflective signatures of the clothes, objects and backgrounds in the reflective domain, the emissive signatures of the persons and objects in the thermal domain, and the additional information brought to the human brain or to ATR thanks to the movements of the targets. The imaging instruments were operated simultaneously and from the same building (but up to 8 m apart, inducing translation and rotation transformation). To be able to take care about the translation and rotation between the sensors some flat geometrical targets (right side in Figure 2; constructed to be seen in every wavelength) were used to enable an extrinsic calibration (registration) of the sensors.

All clothes used in this campaign have been measured spectrally from 400 to 2500 nm. A spectrally calibrated reflectance board (see Figure 2) has been in view for every measured scene and from every sensor. From the reflectance board, images from different sensors are calibrated to each other and directly comparable. A resolution target and an MTF slanted-transition target were used to evaluate the spatial resolution and the sensor sight in different turbulence conditions. A scintillometer acquired the turbulence during the whole campaign. Weather data and light conditions were also acquired. A fisheye camera imaged the cloud configuration over the field continuously on 9th April 2013. Most scenes with humans acting were also video recorded and/or photographed.

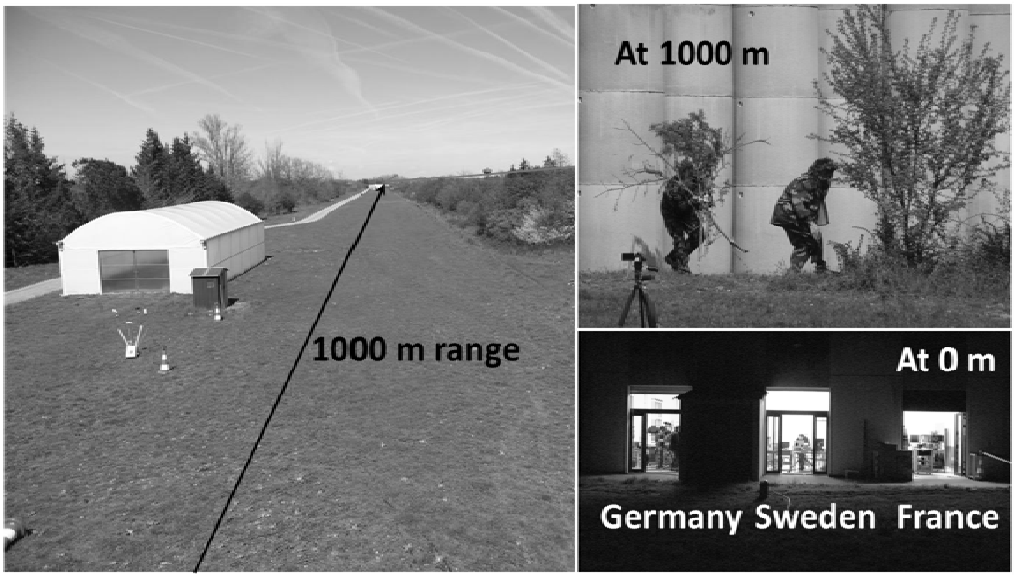

Figure 1. The Pirrène laser range of Oneraoffers a 1040 m range. The targets were placed from 600 to 1000 m from the sensors. Each country used separate rooms which results in some parallax between the sensors.

2.2 Environmental conditions

We were able to perform measurements under a good variety of environmental conditions: clear sky, cloud coverage, mist, heavy thunderstorm and after thunderstorm. These conditions encompassed from solar-noon to evening and night (19:02-19:33 on 8th April 2013, 16:02-22:58 on 9th April, 16:27-00:30 on 10th April and 14:05-20:16 on 11th April). Monday 8th and Tuesday 9th April were cloudy and misty days. Wednesday 10th and Thursday 11th April offered clear sky conditions day and night, except for the thunderstorm at about 18:00 on Thursday 11th April.

A CimelEnerco weather station acquired the following parameters every minute: air temperature Ta (°C), relative humidity RH (%), global irradiance GI (W/m^2), wind speed WS (m/s) and wind direction WD (degree). These data were recorded from Monday 8th April 2013 at 00:00 until Friday 12th April 2013 at 09:00. Figure 3 shows the weather station and the temporal variation of the meteorological data over that period. Figure 4 shows the daily evolution of the atmospheric turbulence along the four days of effective trials. The turbulence measurements correlate with the weather conditions.

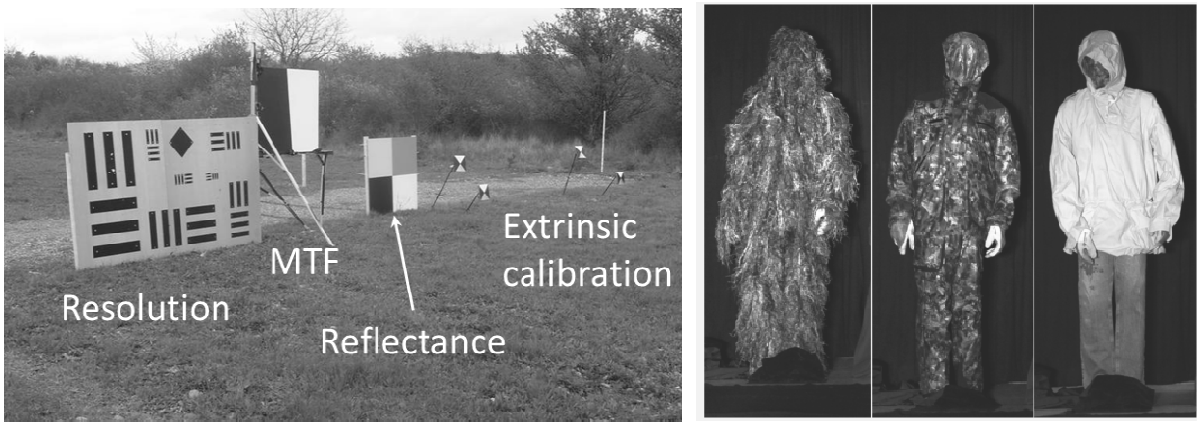

Figure 2.Left: Reference targets used during the trial. Right: Some of clothes used. From left to right: ghillie suit, hunting clothes and white anorak + light-blue jeans.

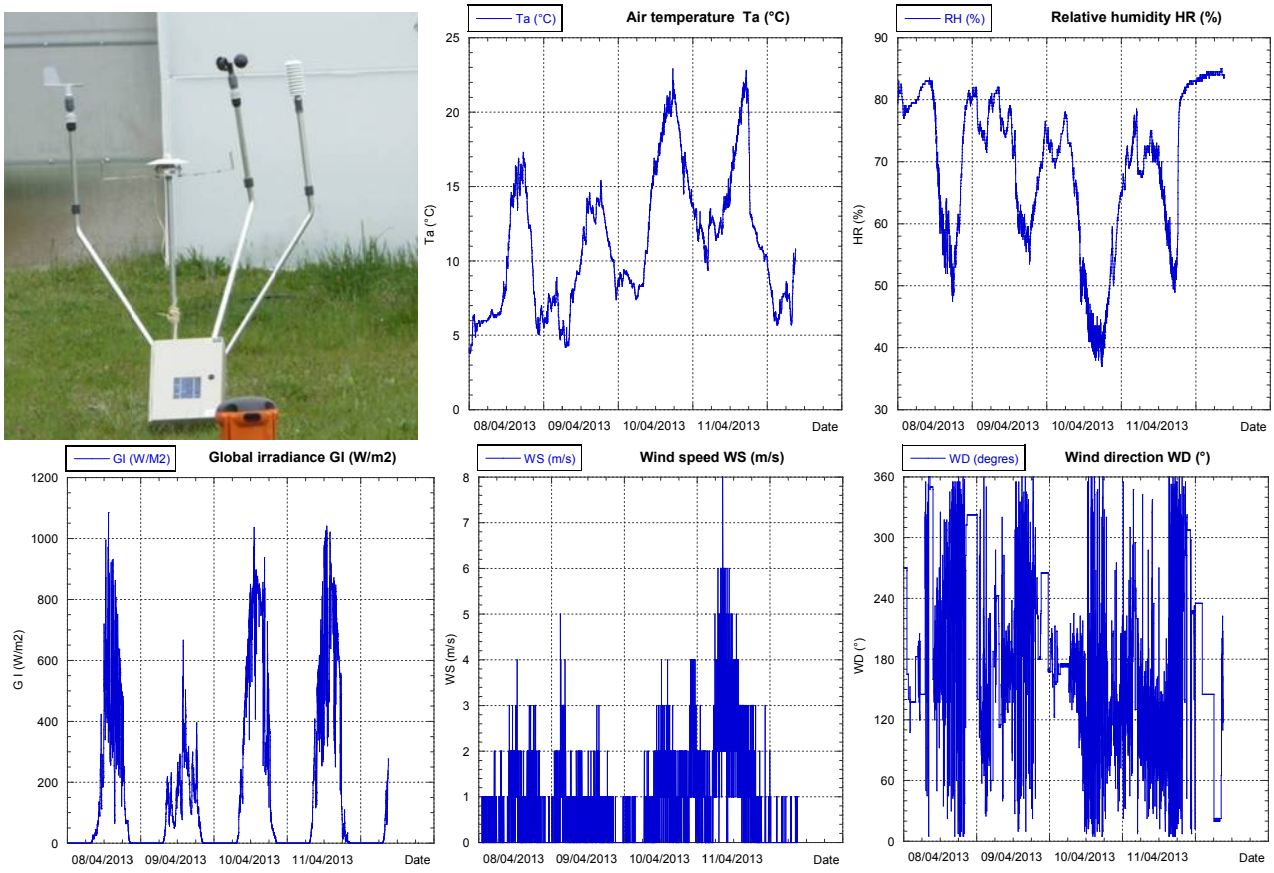

Figure 3.CimelEnerco weather station (top left) and weather measurements from 8th April 2013 (00:00) to 12th April 2013 (09:00): air temperature, relative humidity, global irradiance, wind speed and wind direction (from left to right, top to bottom).

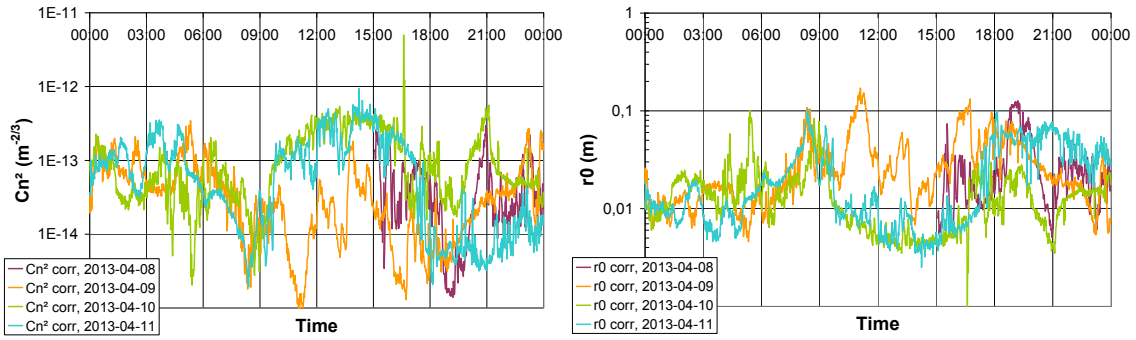

Figure 4: Temporal evolution of the atmospheric turbulence along the trials, measured by a Scintecscintillometer: the structure constant of the optical index fluctuations Cn² (left) and the Fried diameter r0 (right).

2.3 Details of each instrument

During the field trials ten main sensors were operational. The sensors were selected to cover a broad spectral range and as well to operate in both the passive imaging and active imaging regime. A specifications summary of each sensor is given in Table 1. All three active imaging sensors were operating in the NIR-SWIR regime while the passive systems were operating in different bands from the VIS to LWIR.

Figure 5. The three teams sensor setups, from the left: IOSB, FOI and ONERA.

Each research group arranged theirimaging instruments in close vicinity to each other to obtain similar viewing conditions, see Figure 1and Figure 5. There are variations in number of pixels and FOV for the sensors, which gives a variation in number of pixels on the targets. This puts some restrictions on the possibilities for data registration. An example of data collected for similar scenes with all sensors is shown in Figure 6.

The ONERA group operated three instruments. The Gibi is a homemade 2D flash active system working at the wavelength of 1574nm with a 256×256 sensor matrix. For the VIS (Red,Green,Blue) and NIR domain, a sensor called Pelican featured four independent passive sensors. Each of these had a detector array of 4106×4096 pixels, which was the highest number among all the sensors. Although they had the largest format they also had the largest field of view which limited them to have a limited resolution on the targets. ONERA also provided a FLIR cameracovering the LWIR band from 8.0µm to 9.3µm, with a 640×512 array.

FOI provided a commercialactive/passive imaging sensor, model Obzerv ARGC 750. This system operates at the wavelength 808nm with output images of size of 720×480 pixels. The Obzerv can also be operated as a passive system in NIR wavelength region with the same resolution. An eye safety limit of 108m was set by this system due to the high laser pulse energy, up to 330µJ, at a non-eye safe wavelength.

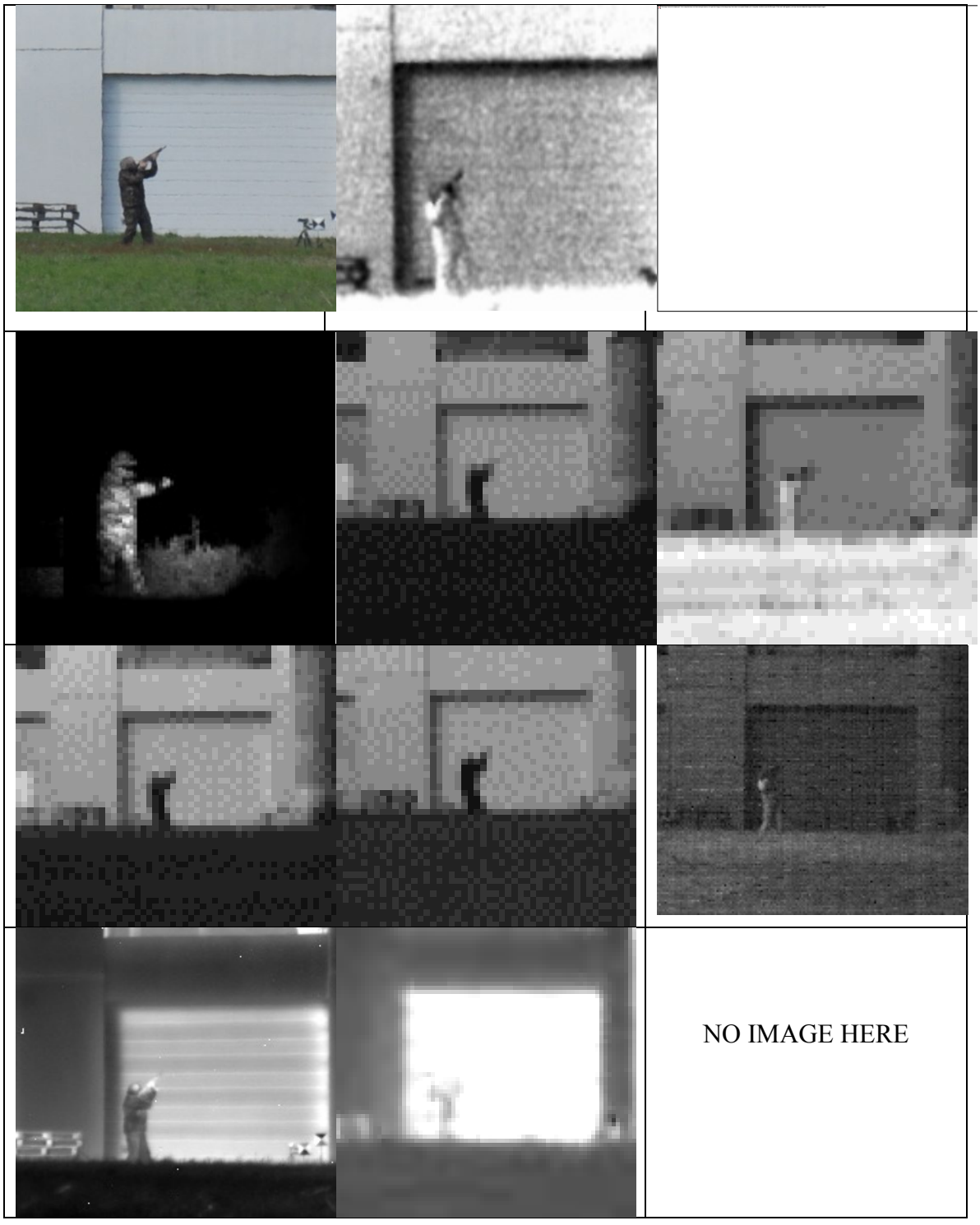

Figure 6: Example of collected data, person dressed in hunting clothes aiming with a replica gun (plastic). From top left to bottom right: Vis, Obzerv (averaged), IOSB's Intevac (averaged), Onera'sGibi, Pelican red, Pelican green, Pelican, blue, Pelican NIR, passive SWIR, MWIR and LWIR.Range 1000m, except for Gibi 600m.

The team from IOSB provided three main sensors covering from SWIR to MWIR. Their active system, used an Intevac, image intensified sensor and operated at 1572nm wavelength with an image output size of 640×480 pixels. Also for the SWIR, a passive sensor from Xenics provided coverage over 0.9µm to 1.7µm with a 640×512 pixel image format. The third sensor from IOSB was a MWIR sensor covering 3.4 – 5.3µm with 640×480 pixels.

Table 1. Summary of the ten sensors used in the field trial.

Instrument	**Active/ Passive**	**Type**	**Wavelength coverage (nm)**	**FoV (mrad)**	**iFoV (µrad)**	**Frame rate (Hz)**	**NOHD (m)**	**eNOHD (m) 7x**
Gibi	Active	2D flash	1574	3 - 8.5	66.4 - 33.2	10	5 - 12	35 - 100
Pelican	Passive	Blue Green Red NIR	452 – 529 512 – 595 623 – 706 780 – 932	250	60	0.25	na	na
FLIR SC7000	Passive	LWIR	*8000 – 9300*	50	80	115	na	na
Obzerv	Active/ Passive	2D flash	808	8.4-146	13.2-12.2	30	20-108	140-756
Intevac	Active	2D flash	1572	17.1×12.9	26	20	2.4	9.6
Xenics	Passive	SWIR	900 – 1700	26.2×20.9	40.3	25	na	na
IR Camera AIM	Passive	MWIR	3400 – 5300	15.4×11.5	22.3	30	na	na

3. EXAMPLES OF DATA FROM THE OBZERV SENSOR

Figure 7shows active image examples of persons with different clothes at 600 meter range. Using the reflectance panel we could derive the apparent reflectance observed in the images and compare that with the laboratory collected spectral curves for the clothes.

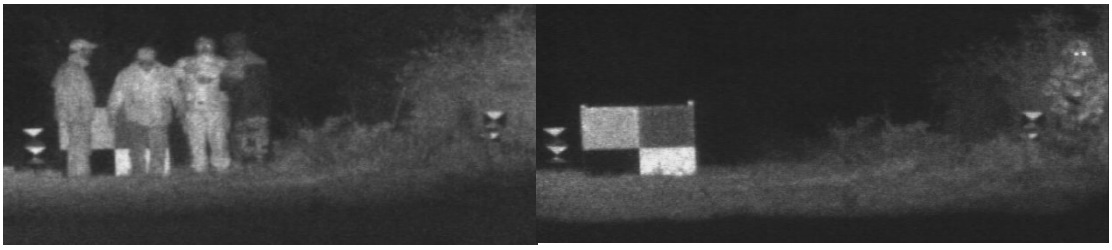

Figure 7. Left active image of persons with different clothes and right the image of a camouflaged persons (to the right) showing the strong retro-reflection from the eyes. Range 600 meters. NOHD (Nominal Ocular Hazardous Distance) 36 meters. The illumination power at 808 nm was 1.1-1.3 W. The 4-section panel had reflectance from high to low of 62, 31,17 and 2.7 % at the 808 nm wavelength. Left image: 2013-04-11 19:03.27, right image19:51:27.

Figure 8 shows the advantage of active imaging to enhance imagery in heavy rain. In Figure 9we illustrate two well-known facts. First, gated viewing can provide strong target-to-background contrast. Second, a silhouette image, when the gate is positioned behind the target, can reveal complementary details, compared to an illumination image with the gate centered on the target. Note how the rifle is more outstanding in the silhouette image than in the illumination image.

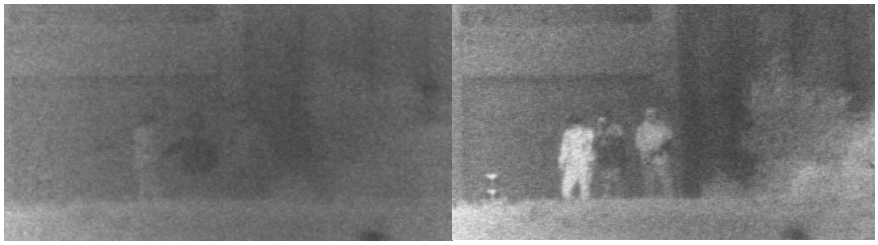

Figure 8.Three persons standing in front of a concrete wall, heavy rain, distance 800m. Left passive and right active image.(Left 2013-04-11, time 18:13:05 and right 2013-04-11, time 18:20:47)

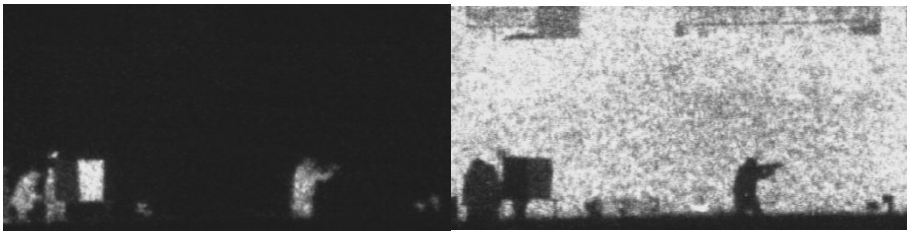

Figure 9.A person and a black/white test target (left part of image) and person aiming with rifle (right), range 1000m. Left image: active illumination in reflectance mode, right: active illumination silhouette mode. (Left 2013-04-10, time 23:13:31 and right time 23:17:40).

4. EXAMPLES OF DATA FROM THE LWIR SENSOR

Figure 10 shows the main characteristics of the LWIR cooled sensor and a photograph of the camera block. Figure below shows LWIR images extracted from two movies corresponding to two different scenarios:

- Man filming with smartphone (scenario 26) during night with no rain and low turbulence (top);
- Man hunting with automatic rifle (scenario 1) during sunny day with no rain and strong turbulence (bottom).

The optical resolution limit of the LWIR camera (due to the diffraction limit and the lens / detector combination) available for the experiment is two to four times higher than those of other sensors (except Pelican). However, the radiometric sensitivity of the instrument provides movies of sufficient quality for using it as a valuable input for evaluating the respective merits and complementarities of active and passive imaging, as well as of the different spectral bands, in the analysis of human activities.

Camera model	FLIR LWIR HgCdTe
Spectral band Δλ (µm)	LWIR - 8.0 µm – 9.3 µm
Detector number Ndx * Ndy	640 * 512
Detector pitch Pdx * Pdy (µm)	16 µm * 16 µm
Sensor frame rate FR (Hz)	25 Hz for the experiment
Focal length / F-number fo (m) / Fno	0.2 m / 2
Sensor field of view FOVx * FOVy (°)	2.9 ° * 2.3 °
Instantaneous field of view ifov (µrad)	80 µrad
Diffraction angular resolution δθdiff (µrad)	104 µrad
Pixel projected at target or GSD (cm)	
D = 600 m	4.8 cm
D = 1000 m	8.0 cm

Figure 10.LWIR cooled sensor characteristics (left) and LWIR camera block along with the blackbody used for non-uniformity corrections (right)

Figure 11.LWIR cooled sensor examples results for two scenarios: night – low turbulence (top) and day – sunny – strong turbulence (bottom).

5. SPECTRAL DISCRIMINATION:ACTIVE/PASSIVE 808 nm VS. ACTIVE 1.5 µm

One of the key questions for the trial was that of spectral discrimination of clothes. We will give some examples comparing active and passive imaging in the NIR vs. SWIR region by using the data from Obzerv with that from the 1.5 µm gated viewing system from IOSB.Figure 12 shows one example of spectral signatures. There is a general tendency that both NIR and SWIR imaging does not preserve the spectral signatures as clear (with such a high contrast) as in the visible wavelength region. Note for example that the blue white pattern from the sweater disappears both in the passive NIR and the active SWIR image. The relatively dark brown jacket appears as light (highly reflective) especially in the active 1.5 µm image. The pattern on the camouflage jacket is visible in the 1.5 µm active image but not so much in the passive NIR image. Another example is given in Figure 13. Again the pattern of the uniform is more or less "washed out" in the passive NIR image as compared with the color or corresponding grey tone image. Note the reverse contrast for the black and grey jacket in the NIR vs. the visible region. The same tendency is seen in Figure 14.

If we look at the laboratory collected reflectance spectra (Figure 15) from the hunting clothes (item A), beige jacket (G) and jeans (item H) we observe that for both 808 nm and 1550 nm, the black-brown-green camouflage pattern intended for the visible is washed out in the NIR and SWIR bands. We also observe that for both 808 nm and 1550 nm the reflectancefor the items G and H are all about 50%. This explains why there seems to be no reflectance contrast in the 808 and 1550 nm images for these clothes. We also note that the contrast between the white and blue parts of the jogging dress completely disappear in the NIR and active SWIR images.

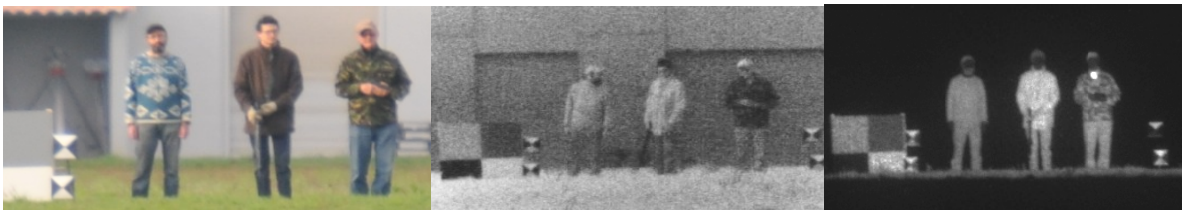

Figure 12. Clothes measured from 600m distance. Left: visual, middle:Obzerv (NIR) in passive mode, right: Intevac 1.5 µm active mode. From left to right in each image: Blue and white sweater, jeans and black cap, 2: brown jacket and jeans (object automatic rifle) 3: hunting jacket D, jeans and beige cap (object gun). (Scenario Test1 2013-09-08 19:15)

Figure 13.Clothes measured from 800m distance. Left: visual, middle:gray scale VIS image, right:passive NIR image. Clothes in each image, from left to right: Ghillie (Item J), 2: Swedish hunting (Item A) and blue cap, 3:Grey jacket (Onera) and jeans. (Scenario 50 2013-04-09 16:14)

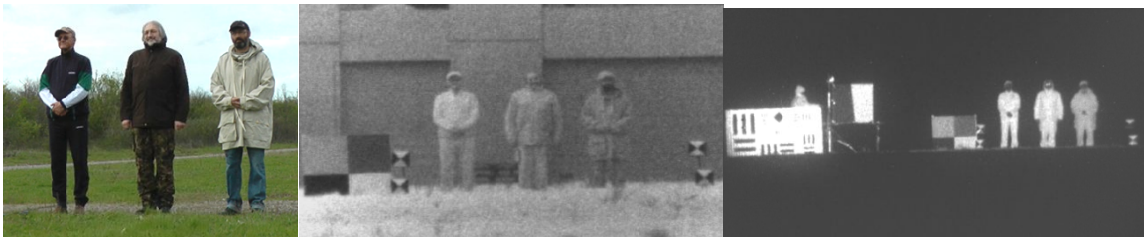

Figure 14.Clothes measured from 800m distance. Left: visual, middle: passive NIR, right:active 1.5 µm. Clothes from left to right in each image: jogging dress, Swedish hunting pants (Item A) and brown jacket, white anorak (Item G) and jeans (Item H). (Scenario 51 2013-04-09 18:03:15)

From Figure 16 we also conclude that the speckle pattern is more dominant for the active 808 nm system as compared with the 1550 nm system. We assume that these speckles are induced by atmospheric turbulence which has a higher effect on shorter wavelength illumination. This speckle noise will limit the identification of clothes and may confuse camouflage from plain-colored ones, except that the speckle noise is not stationary whereas the camouflage patterns of a still target are stationary. This is also illustrated in Figure 17. In Figure 18we observe that grey, red and black clothes appear to have approximately the same brightness for the 1550 nm active image but are more different for the passive 808 nm image.

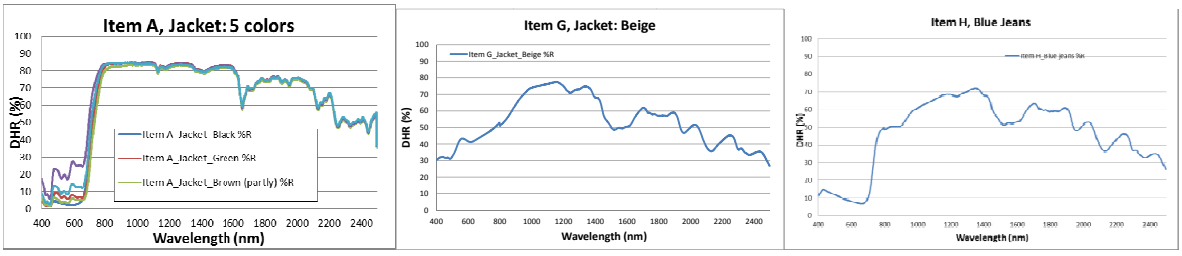

Figure 15. Left to right: reflectance for the hunting clothes (item A), the beige jacket (item G) and the jeans (item H).

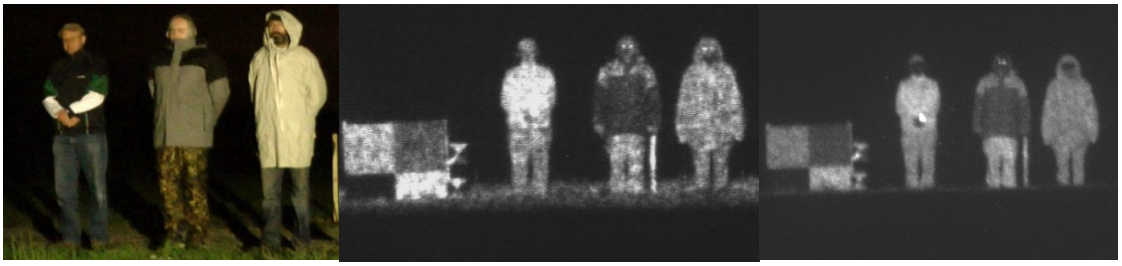

Figure 16. Clothes measured from 800m distance. Left: visual, middle: active NIR image, right: active 1.5 µm. Clothes from left to right in each image:Jogging dress, jeans and beige cap. 2: Grey jacket and Swedish hunting pants (A). 3: White anorak (item G), jeans (item H) and black cap. (Scenario 63, 2013-04-09 22:26:55)

Figure 17.Clothes measured from 800m distance. Left: visual, middle: active NIR image, right: active 1.5 µm. Clothes from left to right in each image: 1: Uniform item F, jeans and beige cap, 2:Swedish hunting clothes and 3: grey jacket, jeans and black cap.(Scenario 60, 2013-04-09 22:10:55)

Figure 18.Clothes measured from 1000m distance. Left: visual, middle: passive NIR, right: active 1.5 µm. Clothes from left to right in each image: Black cotton to the left, red sweater (polyester) in the middle and white (and black) polyester to the right. (Scenario 54, 2013-04-10 18:54:05)

For detection, the target to background contrast is essential. The prospects for detection of clothes in the SWIR region seem promising when we compare typical reflectance curves for clothes (cfFigure 19for representative examples) vs. reflectance of typical terrain and urban background. Clothes including uniforms have generally high reflectance (between 40-60%) in the NIR-SWIR region which is usually higher than what is found in vegetation at least around 1.5 µm. The clothes reflectance in the NIR/SWIR regions will also often be higher than that found in typical urban materials, such as concrete, according to Figure 19. Figure 20 illustrates the contrast of persons with different clothes seen against grass and bushes. The contrast seems more pronounced at 1.5 µm than at 808nm in accordance with the discussion above. This is further exemplified in Figure 21.

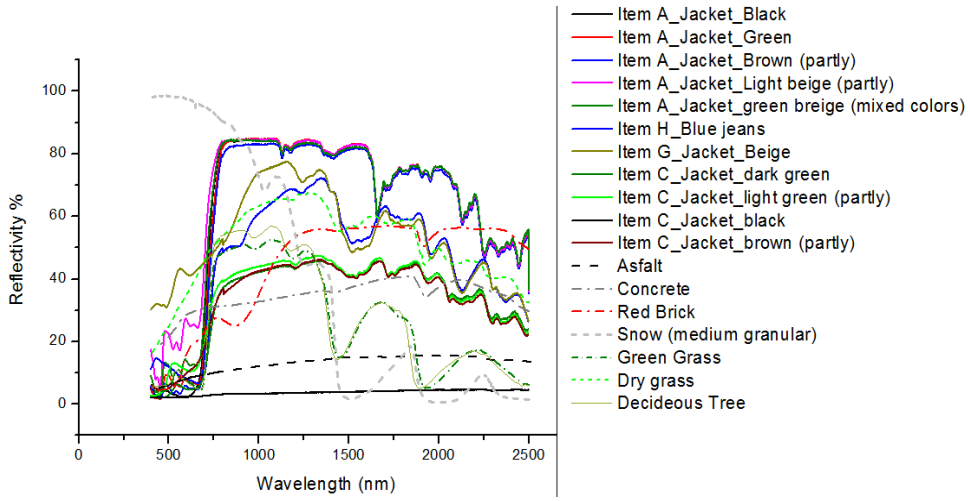

Figure 19. Example of cloth material and terrain background reflectance (Background spectra based on http://speclib.jpl.nasa.gov/).

Figure 20.Clothes compared to background, range 1000m. Left: an active 1.5 µmimage of a crowd against bushes and a concrete wall, middle: persons against the terrain for active 808 nm imaging, right: a person against the terrain at 808 nm. In the latter case the person is well camouflaged against the background. (2013-04-11, time 19:06:39, time 18:51:30, time 17:59:50)

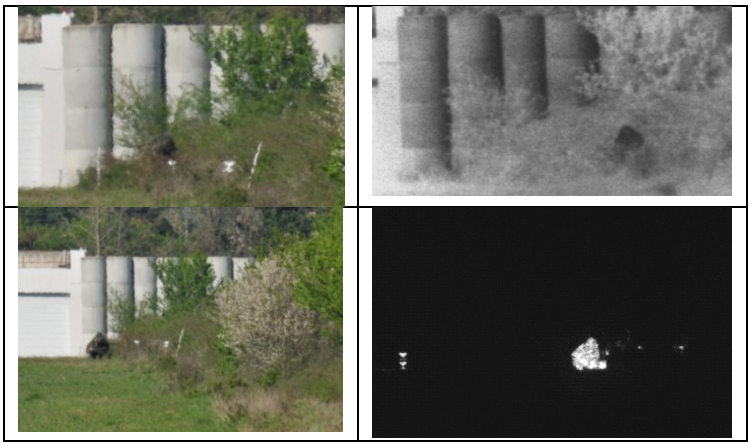

Figure 21.Person in a dark green uniform against bushes and a concrete wall, range 800m. Top left: visual, top right: passive 808 nm image.Bottom left: visual, right: 1550 nm active imaging using a 30 meter gate. (Date 2013-04-11 17:09:07 and 17:15.09)

Figure 22 shows example of the strong 1550 nm active signature in both reflective and silhouette mode. Although we are well aware of the fact that a range gated sensor normally is not a search sensor, the strong signatures of persons as illustrated inFigure 19 and Figure 20 may motivate that it is used for this purpose especially if the search angular sector is limited in size.

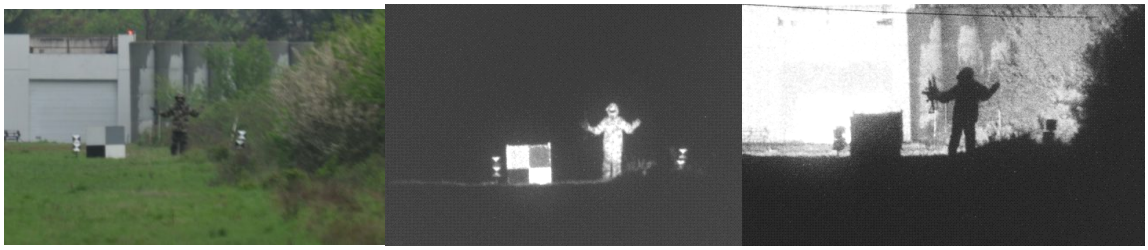

Figure 22.A soldier in uniform with a weapon in his left hand, range 800m. Left: visual, middle: 1550 nm active image in reflective mode, right 1550 nm active image in silhouette mode. The silhouette mode shows a double exposure. (Date 2013-04-11,time 18:26:05)

6. DISCUSSION AND CONCLUDING REMARKS

The measurement campaign that is reported in this paper is part of a joint effort to study active/passive multispectral imaging in the VIS-LWIR regime. Our first objective is to distinguish people against rural and urban backgrounds. The second objective is to distinguish their clothes, hand-held objects and activities. This discussion is based on the presented investigation of a small subset of the data, mainly form the active sensors.

For detection of people, the target to background contrast is essential. The prospect for detection of clothes in the SWIR region seems promising when we compare typical reflectance curves for clothes with the reflectance of typical terrain and urban background. Clothes including uniforms have generally high reflectance (between 40-60%) in the NIR-SWIR region which is usually higher than what is found in vegetation (at least around 1.5 μm). The clothes reflectance in the NIR/SWIR regions will also often be higher than that found in typical urban materials, such as concrete. The contrast of persons with different clothes seen against grass and bushes seems more pronounced at 1.5 μm than at 808nm, which is due to the lower reflectance at 1.5 μm caused by the water content in the vegetation.

One of the key questions is that of spectral discrimination of different clothes for different wavelength bands. Examples comparing active and passive imaging in the NIR vs. SWIR region by comparing the data from 808nmgated viewing Obzerv with that from the 1.5 μm gated viewing system from IOSB have been shown.There is a general tendency that both NIR and SWIR imaging do not preserve the spectral signatures with such a high contrast as in the visible wavelength region. For some clothes the patterns disappear both in the passive NIR and the active SWIR image while on other clothes the pattern is visible in the 1.5 μm active image but not so much in the passive NIR image. Further, some dark clothes appear as light (highly reflective), especially in the active 1.5 μm image. We also noted the reverse contrast for the black and grey jacket in the NIR vs. the visible region. We also observed that for both 808 nm and 1550 nm the reflectancefor thecotton anorak and jeans (items G and H) are all about 50%. This explains why there seem to be no reflectance contrast in the 808 and 1550 images for these clothes. We also note that the white and blue parts of the jogging dress (synthetic fiber) completely disappear in the NIR and active SWIR images. This probably depends on both the material in the clothes (cotton, wool, synthetic fiber etc.), surface treatment and on the spectral signatures of the added colors. The clothes that we have been investigating are designed to “look good” in the visual range.

We also conclude that some observed speckle patterns seem to be more dominant for the active 808 nm system as compared with the 1550 nm system. We assume that these speckles are induced by atmospheric turbulence which has a higher effect on shorter wavelength illumination. This speckle noise will limit the identification of clothes and may confuse camouflage from plain-colored ones. This might be compensated with longer measurement times on the target, as the speckle noise is not stationary whereas the camouflage patterns of a still target are stationary.

We are well aware of the fact that a range gated sensor normally is not a search sensor. We still would like to note that the strong signatures of persons in silhouette mode may motivate to use it for this purpose especially if the search angular sector is limited in size. Further, objects that persons are holding in their hands are more outstanding in the silhouette image.

The amount of collected images from different optical sensors is substantial and needs future analysis. These images together with environmental data will be used for further studies in two main areas. The high-resolution data will be used for further analysis of spectral signatures. The data where one or several persons perform actionsand/or hold different objects will most preferably be used for operator tests [31, 32].

7. ACKNOWLEDGEMENTS

The Swedish participations in the field trial and the analysis work have been funded by the Swedish armed forces FoT-program and the Swedish Defence Material Administration (FMV), which we hereby greatly acknowledge.The laser-range, as well as the French participations in the field trial and in the analysis work has been funded by ONERA.

REFERENCES

1. O. Steinvall, J. Ahlberg, H. Larsson, D. Letalick, D. Hamoir, L. Hespel, Y. Boucher, P. Déliot, P. Lutzmann, E. Repasi, G. Ritt, "Active Imaging (ACTIM)", Report to the European Defence Agency , (EDA ref: 09-R&T-008), 2011, restricted.
2. D. Hamoir, L. Hespel, Y. Boucher, P. Déliot, O. Steinvall, J. Ahlberg, H. Larsson, D. Letalick, P. Lutzmann, E. Repasi, G. Ritt," Results of ACTIM, an EDA study on Spectral Laser Imaging", Proc. SPIE. 8186, V 81860M (2011).
3. O. Steinvall, I. Renhorn, J. Ahlberg, H. Larsson, D. Letalick, E. Repasi, P. Lutzmann, G. Anstett, D.Hamoir, L. Hespel, Y. Boucher ,"ACTIM: An EDA initiated study on spectral active imaging", Proc. SPIE 7835, 78350C, (2010).
4. A.B. Gschwendtner and W.E. Keicher, "Development of Coherent Laser Radar at Lincoln Laboratory", Linc. Lab. J. 12 (2), 2000, pp. 383–396.
5. M. L. Nischan, R. M. Joseph, J. C. Libby, and J. P. Kerekes, "Active Spectral Imaging", Lincoln Laboratory Journal, 14(1):131-144 (2003).
6. L. Le Hors, P. Hartemann, and S. Breugnot, "Multispectral polarization active imager in the visible band", Proc. SPIE, Vol. 4035, pp. 380–389 (2000).
7. L. Morvan, M. Alouini, A. Grisard, E. Lallier, and D. Dolfi, "Two optronic identification techniques: lidar-radar and multispectral polarimetric imaging", Proc. SPIE, Vol. 5613, pp.76-87 (2004).
8. M. Alouini, F. Goudail, P. Réfrégier, A. Grisard, E. Lallier, and D. Dolfi, "Multispectral polarimetric imaging with coherent illumination: towards higher image contrast", Proc. SPIE, Vol. 5432, (2004).
9. M. Alouini, F. Goudail, A. Grisard, J. Bourderionnet, D. Dolfi, I. Baarstad, T. Løke, P. Kaspersen, and X. Normandin, "Active polarimetric and multispectral laboratory demonstrator: contrast enhancement for target detection", Proc. SPIE, Vol. 6396 (2006).
10. Y. Wang, Y. Wang, and H. Q. Lea, "Multi-spectral mid-infrared laser stand-off imaging", Optics Express, Vol. 13, No. 17 (2005).
11. D. J. M. Stothard, M. H. Dunn, and C. F. Rae, "Hyperspectral imaging of gases with a continuous-wave pump-enhanced optical parametric oscillator", Optics Express, Vol. 12, No. 5 (2004).
12. C. R. Howle, D. J. M. Stothard, C. F. Rae, M. Ross, B. S. Truscott, C. D. Dyer, and M. H. Dunn, "Active Hyperspectral Imaging System for the Detection of Liquids", Proc. SPIE, Vol. 6954 (2008).
13. J. F. Andersen, J. Busck, and H. Heiselberg, "Pulsed Raman fiber laser and multispectral imaging in three dimensions", Appl. Opt., Vol. 45, No. 24 (2006).
14. M. A. Powers and C. C. Davis, "Optical Signatures for Autonomous Mobility", Proc. SPIE, Vol. 7324 (2009).
15. M.A. Powers and C. C. Davis, "Spectral LADAR: active range-resolved three dimensional imaging spectroscopy", Applied Optics, Vol. 51, No. 10, pp. 1468-1478, (2012).
16. S. Kaasalainen, T. Lindroos, and J. Hyyppä, "Toward hyperspectrallidar - Measurement of spectral backscatter intensity with a supercontinuum laser source", IEEE Geosci. Remote Sens. Lett., 4, 211-215 (2007).
17. T. Hakala, J. Suomalainen, S. Kaasalainen, and Y. Chen, "Full waveform hyperspectralLiDAR for terrestrial laser scanning", Optics Express, March 2012 , Vol. 20, No. 7, pp. 7119-7126 (2012).
18. J.I. Park, M.H. Lee, M. D. Grossberg, and S. K. Nayar, "Multispectral Imaging Using Multiplexed Illumination", IEEE 11th International Conference on Computer Vision, 2007.
19. Moyer, S., Hixson, J.G, Edwards, T.C, Krapels, K., "Probability of identification of small hand-held objects for electro-optic forward-looking infrared systems", Optical Engineering 45 (6), 063201, (2006).
20. Krapels, K., Driggers, R.G., Teaney, B., Halford, C., "Handheld threat object identification performance of 2-D visible imagery versus 3-D visible imagery", Optical Engineering 45 (6), 063202, (2006).
21. Krapels, K., Driggers, R.G., Vollmerhausen, R.H., Kopeika, N.S., Halford, C.E., "Atmospheric turbulence modulation transfer function for infrared target acquisition modeling", Opt. Eng. 40(9) pp. 1906–1913 (2001).

22. Espinola, R.L., Aghera, S., Thompson, R., and Miller, J., “Turbulence degradation and mitigation performance for handheld weapon ID”, Proc. of SPIE Vol. 8355, 83550S (2012).
23. R. G. Driggers, E.L. Jacobs, R.H. Vollmerhausen, B. O'Kane, M. Self, S. Moyer, J.G. Hixson, G. Page, K. Krapels, D. Dixon, R. Kistner, J. Mazz, “Current infrared target acquisition approach for military sensor design and wargaming”,Proc. SPIE.Vol. 6207, 620709 (2006).
24. T. Maurer, D. L. Wilson and R. G. Driggers, “Search and detection modeling of military imaging systems”, Optical Engineering 52 (4), 041108 (2013).
25. Espinola, R. L., Jacobs, E. L., Halford, C. E., Vollmerhausen, R. H. and Tofsted, D. H., “Modeling the target acquisition performance of active imaging systems”, Opt. Express 15 (7), 3816-3832 (2007).
26. V. Farley, M. Kastek, M. Chamberland, T. Piątkowski, P. Lagueux, R. Dulski, P. Trzaskawka, “Multispectral and hyperspectral advanced characterization of soldier's camouflage equipment”,Proc. SPIE. vol. 8743, 87431P, (2013).
27. P. Zhou, F. Wang, H. Zhang, M. Xue, “Camouflaged target detection based on visible and near infrared polarimetric imagery fusion”, Proc. SPIE. 8194, 81940Y (2011).
28. M.A.Hogervorst, A. Toet, P. Jacobs, “Design and evaluation of (urban) camouflage”, Proc. SPIE. 7662, 766205 (2010).
29. Turaga, P., Chellappa, R., Subrahmanian, V.S., Udrea, O., “Machine Recognition of Human Activities: A survey”, IEEE Transactions on Circuits and Systems for Video Technology, Vol. 18, No. 11, (2008).
30. O’Connor, J. D. , O’Kane, B. L. , Royal, C. K., Ayscue, K. L. , Bonzo, D. E. and Nystrom, B. M., “Recognition of human activities using handheld thermal systems”, Proc. SPIE3394, pp. 51–61 (1998).
31. O. Steinvall, M. Elmqvist, T. Chevalier, “Identification of handheld objects and human activities in active and passive imaging” Proc. SPIE. 8542, 854206 (2012).
32. O. Steinvall, M. Elmqvist, T. Chevalier, O. Gustafsson, “Active and passive SWIR and NIR imaging for horizontal and slant paths close to ground”, to be published in Applied Optics.
33. U. Adomeit, “Infrared detection, recognition and identification of handheld objects”,Proc. SPIE vol. 8541, 85410O (2012).